



REGULAR ARTICLE

Nanoparticles of ZnO/ZnS: Electrochemical Synthesis, Analysis and Prospective Applications

O.V. Smitiukh\* , O.V. Marchuk, O.M. Yanchuk, Yu.O. Khmaruk, D.S. Zhernov

Lesya Ukrainka Volyn National University, 43025 Lutsk, Ukraine

(Received 19 December 2023; revised manuscript received 17 February 2024; published online 28 February 2024)

This article presents a detailed study on the electrochemical synthesis, analysis, and potential applications of nanoparticles composed of zinc oxide (ZnO) and zinc sulfide (ZnS); the electrochemical method of obtaining ZnO/ZnS nanoparticles from a solution using two-electrode synthesis and zinc anodization is described. Sodium chloride and thiourea were used as the electrolyte; the concentration ranges of sulfur-containing substance was investigated, under which only zinc sulfide can be obtained. The influence of thiourea concentration on the particle thickness and composition of the electrolysis products in an aqueous solution of sodium chloride with a soluble zinc anode was studied for the first time. X-ray diffraction was employed to analyze the structural properties and thickness of the nanoparticles. The products of zinc anodization are nanoscale zinc oxide and zinc sulfide. With an increase in the thiourea content, the thickness of the formed particles decreases. It was found that at the lowest thiourea concentrations, mainly zinc oxide is formed, while at the highest concentrations, mainly zinc sulfide is formed. Increasing the concentration of thiourea is accompanied by the transformation of the wurzite modification of ZnO into sphalerite and the substitution of oxygen atoms with sulfur atoms. ZnS particles (1.3-3.6 nm) are significantly thinner than ZnO particles (7-29 nm). The synthesized nanoscale powders of zinc oxide, zinc sulfide, and their mixtures can be used for the production of semiconductor devices. The article discusses the potential applications of these nanoparticles in various fields such as photocatalysis, sensors, and energy storage devices. Overall, this study provides valuable insights into the synthesis, characterization, and potential applications of ZnO/ZnS nanoparticles, highlighting their promising prospects in nanotechnology.

**Keywords:** Electrochemical Synthesis, Nanopowder, Zinc Oxide, Zinc Sulfide, Structure.

DOI: [10.21272/jnep.16\(1\).01024](https://doi.org/10.21272/jnep.16(1).01024)

PACS numbers: 81.07.Wx, 82.45.Aa

1. INTRODUCTION

The development of nanotechnology has opened up new opportunities for creation of materials with unique properties and applications. One such material is zinc oxide (ZnO) [1] and zinc sulfide (ZnS) [2] nanoparticles, which have attracted significant attention due to their potential applications in various fields, including optoelectronics, photocatalysis, and sensors. The electrochemical synthesis of ZnO/ZnS nanoparticles has emerged as a promising method for producing these materials with high purity and controlled size and shape. This article discusses the challenges and future directions in the development of the materials for various applications.

In recent years, zinc oxide is a widely used metal oxide material because of its unique physical and chemical properties such as high chemical [3] and mechanical stability [4], broad range of radiation absorption [5], high piezo-catalytic activity [6], electro chemical coupling coefficient [7], non-toxic nature etc.

ZnO is a semiconductor in group II-VI (a broad energy band of 3.37 eV) at room temperature. ZnO (NPs) is low toxicity, low cost and an excellent material due to their crystal structure, size and stability [8].

In the work, we presented the results of obtaining double-powder ZnO/ZnS nanoparticles that can be used for perspective applications.

2. EXPERIMENTAL DETAILS

Nanoscale sediments was obtained by electrolysis of an aqueous solution of sodium chloride and thiourea in galvanostatic mode (current strength 2.04 A,  $t_{const} = 90$  °C) with identical zinc plates (anode) and coal rods (cathod) with an area of electrode 5 cm<sup>2</sup>. For the synthesis of ZnO and ZnS, 1M solution of sodium chloride and thiourea (0.25 M ÷ 3,0 M with a step in 0.25 M) has been used. The voltage varied from 5.6 to 6.6 V.

Table 1 – The details of experiment

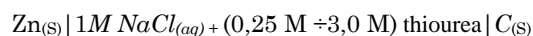
No	[CH <sub>4</sub> N <sub>2</sub> S], M	Current, V
1	0.25	6.0
2	0.5	6.0
3	0.75	5.9
4	1.0	5.6
5	1.25	6.6
6	1.5	6.4
7	1.75	6.0
8	2.0	5.9
9	2.25	6.4
10	2.5	5.8
11	2.75	6.3
12	3.0	6.3

\* Correspondence e-mail: [Smitiukh.Oleksandr@vnu.edu.ua](mailto:Smitiukh.Oleksandr@vnu.edu.ua)

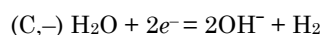
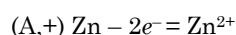


The starting materials were transferred into a measuring flask (200 mL) and filled with water to more than half of its volume. The mixture was then heated to the experimental temperature (90 °C) for the dissolution of the electrolysis components, and water was added up to the mark on the flask. The resulting solution was poured into a 400 mL flask, where electrodes (a zinc plate and a carbon rod) were placed. The electrolyzer (a beaker with the electrolyte solution, a neodymium magnet, electrodes submerged in the solution, a thermocouple, and a regular mercury thermometer) was immersed in a thermostat that maintained a constant temperature of 90°C, and connected to a constant current source B5-46 or B5-49. The current and voltage on the electrolyzer were monitored by an ammeter and voltmeter. The experimental duration was 20 minutes, which was the same for all experiments. The setup for electrochemical synthesis is shown in Fig. 2.

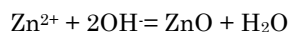
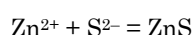
In the electrolytic cell



the following half-reactions occur on the electrodes:



It is worth noticing that the total equations for electrolysis then reads:



This reaction may be used in the synthesis of semiconductor materials, such as zinc oxide and zinc sulfide nanoparticles, which have application in optoelectronic, solar cells, and photocatalysis.



Fig. 1 – Installation for electrochemical synthesis of nanopowders

After cooling, the solution was decanted from the glass and filled with distilled water. After a day, the solution was decanted again and filled with distilled water. After another decantation, distilled water was added again and left for another day before decanting the water. After the final washing and decantation, the contents of the glass were poured into a Petri dish and left in a drying cabinet for a day at a temperature of 50 °C. The dried powders were sent for analysis to an X-ray laboratory.

### 3. DISCUSSION

In Scherrer' first work [8] on particle size determination, Paul Scherrer proposed the following formula in 1918:

$$D = K\lambda/(\beta\cos\theta),$$

where  $D$  is the average particle size in nm;  $K$  is a constant whose value depends on the shape of the particle, in our case it is 0.941;  $\beta$  is determined as half the width of the maximum peak measured in radians;  $\lambda$  is the wavelength of the X-ray radiation, which is 0.15418 nm;  $\theta$  is the diffraction angle for the maximum.

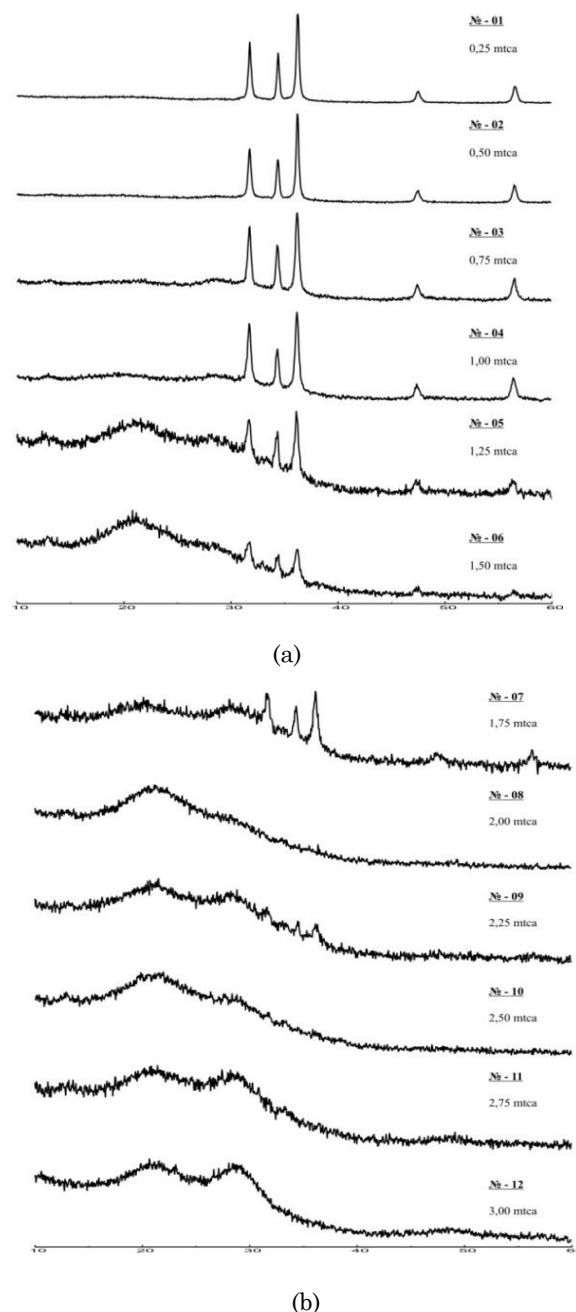


Fig. 2 – (a) Diffraction patterns of powder samples 1-6 obtained with TCA concentrations ranging from 0.25 to 1.5 M; (b) Diffraction patterns of powder samples 7-12 obtained with TCA concentrations ranging from 1.75 to 3.0 M

The diffraction patterns shown in Figs. 2 were processed using Powder Cell and X'pert Highscore Plus software for identification and determination of the quantitative composition of phases. It was found that samples 1-7 contain zinc oxide crystals, with samples 1-5 exhibiting mainly the wurzite structure  $\beta$ -ZnO (from 97.5 to 100 %). In samples 6-7, the sphalerite  $\alpha$  modification  $\alpha$ -ZnO (from 25 to 35 %) increases. Starting from sample 2, a halo appears at an angle of  $2\theta$  28-29°, which may indicate the presence of zinc sulfide. In samples 8-12, the intensity of zinc oxide peaks is low, and the size of the zinc sulfide halo increases, reaching maximum values for samples 11-12. It can be concluded that the content of zinc oxide in samples 5-12 begins to decrease, while zinc sulfide increases. The presence of a halo indicates small particle sizes, primarily zinc sulfide.

According to the results of diffraction pattern analysis, the main product of zinc anodization with TCA concentrations up to 1.75 M is  $\beta$ -ZnO. At higher TCA concentrations, a mixture of zinc oxide and zinc sulfide is present, with zinc sulfide prevailing at high TCA contents.

It was found that samples 1-7 contain zinc oxide crystals, with samples 1-5 exhibiting mainly the wurzite ( $P6_3mc$ ) structure of zinc oxide (from 97.5 to 100 %) (Fig. 4). In samples 6-7, atom rearrangement occurs, leading to an increase in cell filling coefficient and as a result, more electronegative particles are localized around zinc atoms, forming an octahedral sextet (Fig. 4). The content of the sphalerite modification ( $Fm-3m$ ) increases for zinc oxide samples (from 25 to 35 %). In addition, starting from sample 2, the formation of a halo in the range of angles  $2\theta$  28-29° becomes noticeable, which may indicate a decrease in particle size and the appearance of zinc sulfide. Since there is no clear separation of peaks, it can be assumed that this pattern is present for both the wurzite and sphalerite modifications. This is because the coordination environment changes to tetrahedral when oxygen atoms are replaced by sulfur atoms in sphalerite (Fig. 3).

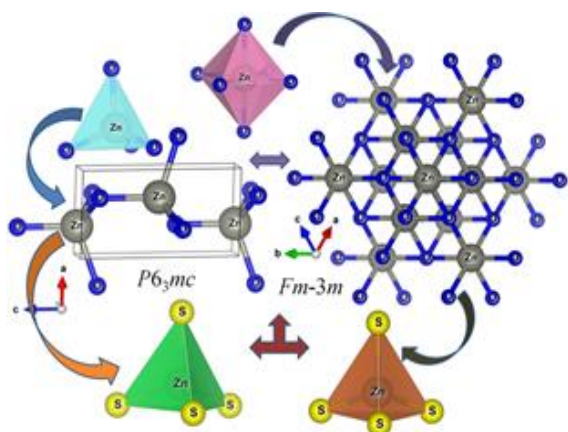


Fig. 3 – Structural transformations in the synthesized samples

This leads to cell densification and particle size reduction. In samples 8-12, the intensity of zinc oxide peaks is low, and the size of the zinc sulfide halo increases, reaching maximum values for samples 11-12. It can be concluded that the content of zinc oxide in samples 5-12 begins to decrease, while zinc sulfide increases.

Table 2 – Results of determining the average thickness of zinc oxide particles.

No	$2\theta_1-2\theta_2$	$\beta$	$2\theta$	$\cos\theta$	[TCA], M	D, nm
1	0.30	0.00523	36.25	0.9503	0.25	29.2
2	0.32	0.00559	36.25	0.9504	0.50	27.3
3	0.39	0.00681	36.20	0.9507	0.75	22.4
4	0.40	0.00698	36.15	0.9507	1.00	21.9
5	0.43	0.00751	36.10	0.9508	1.25	20.3
6	0.58	0.01012	36.10	0.9508	1.50	15.1
7	0.49	0.00855	36.10	0.9508	1.75	17.8
8	0.54	0.00943	36.10	0.9508	2.00	16.2
9	0.61	0.01065	36.10	0.9508	2.25	14.3
10	0.49	0.00852	36.30	0.9502	2.50	17.9
11	0.80	0.01396	36.40	0.9500	2.75	10.9
12	0.30	0.00524	36.25	0.9501	3.00	6.9

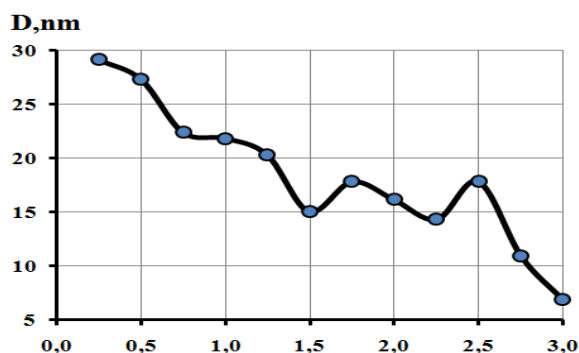


Fig. 5 – Dependence of the thickness of ZnO particles on the concentration of TCA

Table 3 – The effect of TCA concentration on the thickness of zinc sulfide particles

No	$2\theta_1-2\theta_2$	$\beta$	$2\theta$	$\cos\theta$	[TCA], M	D, nm
1	2.40	0.0419	28.65	0.9689	0.25	3.57
2	2.37	0.0414	28.15	0.9699	0.50	3.62
3	2.54	0.0443	28.35	0.9696	0.75	3.38
4	3.04	0.0531	28.60	0.9690	1.00	2.82
5	3.67	0.0641	28.20	0.9699	1.25	2.34
6	3.90	0.0681	28.11	0.9701	1.50	2.20
7	4.33	0.0756	28.11	0.9701	1.75	1.98
8	5.41	0.0944	28.15	0.9699	2.00	1.58
9	5.07	0.0885	28.80	0.9686	2.25	1.69
10	6.10	0.1060	28.21	0.9699	2.50	1.41
11	6.27	0.1090	28.02	0.9703	2.75	1.37
12	6.76	0.1180	28.20	0.9699	3.00	1.27

As can be seen from Table 3 and Fig. 6, the average thickness of particles decreases with an increase in TCA concentration from 3.6 to 1.3 nm.

The main product of zinc anodization at low concentrations of TCA (0.5 M) is  $\beta$ -ZnO, and the second most abundant is  $\alpha$ -ZnO, with a small amount of zinc sulfide present. At TCA concentrations above 1.75 M, zinc sulfide begins to dominate. With an increase in TCA concentration, there is a gradual transformation of  $\beta$  and  $\alpha$ -ZnO structures into  $\beta$  and  $\alpha$ -ZnS structures. The thickness of both zinc oxide and zinc sulfide particles decreases with increasing TCA concentration, as calculated from the Scherrer method diffraction patterns.

All obtained deposits consist of nanosized particles, with particle sizes decreasing from 29 to 7 nm for zinc oxide and from 3.6 to 1.3 nm for zinc sulfide with increasing TCA concentration.

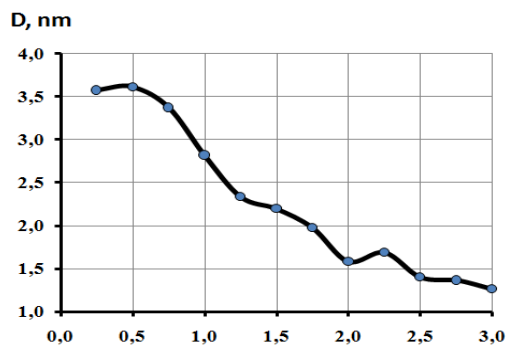


Fig. 6 – Dependence of the thickness of ZnO particles on the concentration of TCA

#### 4. CONCLUSIONS

In conclusion, the study investigated the effect of TCA concentration on the phase composition and particle

thickness of the powder product synthesized by zinc anodization with a carbon cathode under constant current density, temperature, and electrolyte concentration. X-ray diffraction analysis revealed that the powders consisted of zinc oxide and zinc sulfide, with zinc oxide dominating at lower TCA concentrations and zinc sulfide dominating at higher concentrations. The thickness of both types of particles decreased with increasing TCA concentration, and there was a gradual replacement of oxygen atoms in  $\beta$  and  $\alpha$ -ZnO structures with sulfur atoms. The electrochemical synthesis of ZnO/ZnS nanoparticles has been successfully achieved through a simple and cost-effective method. The synthesized nanoparticles were characterized by various analytical techniques, which confirmed their size, morphology, and structural properties. These nanoparticles have potential applications in various fields such as photocatalysis, optoelectronics, and biomedicine.

#### REFERENCES

- O.M. Yanchuk, J. Ebothé, A.M. El-Naggar, A. Albassam, L.V. Tsurkova, O.V. Marchuk, G. Lakshminarayana, S. Tkaczyk, I.V. Kityk, A.O. Fedorchuk, O.M. Vykhryst, I.V. Urubkov, *Physica E* **86**, 184 (2017).
- O.M. Yanchuk, L.V. Tsurkova, O.V. Marchuk, I.V. Urubkov, M. Kolcun, K.M. Rusek, A.M. El Naggar, A.A. Albassam, *Mater. Lett.* **169**, 131 (2016).
- S. Heinonen, J.-P. Nikkanen, E. Huttunen-Saarivirta, E. Levänen, *Thin Solid Films* **638**, 410 (2017).
- J. Germán Soldano, M. Franco Zanotto, M. Marcelo Mariscal, *RSC Adv.* **5**, 43563 (2015).
- E. Casamassa, A. Fioravanti, M. Mazzocchi, M. Cristina Carotta, M. Giulia Faga, *Tribology Int.* **142**, 105984 (2020).
- Q. Nie, Y. Xie, J. Ma, J. Wang, G. Zhang, *J. Clean. Prod.* **242**, 118532 (2020).
- T. Jsung-Ta, W. Sean, *Sensor. Mater.* **31** No 2, 421 (2019).
- K.V. Bhooshan, P Paik, *Adv. Mater. Lett.* **8**, 493 (2017).
- P. Scherrer, Nachr. Ges. Wiss. Göttingen, *Math-Phys. Kl.* **2**, 98 (1918).

### Наночастинки ZnO/ZnS: електрохімічний синтез, аналіз та перспективи застосування

О.В. Смітюх, О.В. Марчук, О.М. Янчук, Ю.О. Хмарук, Д.С. Жернов

Волинський національний університет імені Лесі Українки, 43025 Луцьк, Україні

У цій статті представлено детальне дослідження електрохімічного синтезу, аналіз та потенційне застосування наночастинок, що складаються з оксиду цинку (ZnO) і сульфїду цинку (ZnS); описано електрохімічний метод отримання наночастинок ZnO/ZnS з розчину за допомогою двоелектродного синтезу та анодування цинку. Як електроліт використовували хлорид натрію і тіосечовину; досліджено діапазони концентрацій сірковмісної речовини, за яких можна отримати лише сульфїд цинку. Вперше досліджено вплив концентрації тіосечовини на товщину частинок і склад продуктів електролізу у водному розчині хлориду натрію з розчинним цинковим анодом. Для аналізу структурних властивостей і товщини наночастинок використовували метод рентгенівської дифракції. Продуктами анодизації цинку є нанорозмірні оксид цинку та сульфїд цинку. Зі збільшенням вмісту тіосечовини товщина утворених частинок зменшується. Встановлено, що при найнижчих концентраціях тіосечовини утворюється в основному оксид цинку, а при найвищих – переважно сульфїд цинку. Підвищення концентрації тіосечовини супроводжується перетворенням вюрцитової модифікації ZnO в сфалерит із заміщенням атомів кисню на атоми сірки. Частинок ZnS (1,3-3,6 нм) значно тонші за частинки ZnO (7-29 нм). Синтезовані нанорозмірні порошки оксиду цинку, сульфїду цинку та їх суміші можуть бути використані для виробництва напівпровідникових приладів. У статті обговорюється потенційне застосування цих наночастинок у різних галузях, таких як фотокаталіз, сенсори та пристрої зберігання енергії. Загалом це дослідження дає цінну інформацію про синтез, характеристику та потенційне застосування наночастинок ZnO/ZnS, підкреслюючи їхні багатобіляючі перспективи в галузі нанотехнологій.

**Ключові слова:** Електрохімічний синтез, Нанопорошок, Оксид цинку, Сульфїд цинку, Структура.